Polyurethane–poly(methyl methacrylate) interpenetrating polymer networks

M. Akay*
Department of Mechanical and Industrial Engineering, University of Ulster at Jordanstown, Newtownabbey BT37 0QB, UK

and S. N. Rollins
Boxmore Plastics Ltd, Containers Division, Lurgan BT66 7JW, UK
(Received 25 March 1992; revised 26 June 1992)

A variety of simultaneous and sequential interpenetrating polymer networks (IPNs) based on a polyurethane (PU) network and poly(methyl methacrylate) (PMMA) in linear and network forms were evaluated in terms of dynamic and static mechanical behaviour. IPNs of mid-range composition produced broad tan δ peaks with significant intensities at room temperature to influence elongation to failure. Unusually high elongations at failure were recorded in the simultaneous IPNs due to improved homogeneity in the distribution of the component polymers. The patterns of behaviour of the elastic modulus, hardness and glass transition temperature suggest the occurrence of phase inversion in the simultaneous IPNs and dual-phase continuity in the sequential IPNs. Synergism was experienced in various IPN properties with maximum improvements occurring in the PU/PMMA composition range 30/70 to 40/60.

(Keywords: interpenetrating polymer networks; polyurethane; poly(methyl methacrylate); tan δ; glass transition temperature; phase inversion; phase continuity; fracture surfaces; elastic modulus; hardness; tensile strength)

INTRODUCTION

An interpenetrating polymer network (IPN) is generally defined as being produced between polymers when at least one polymer is synthesized and/or crosslinked in the immediate presence of the other. This results in the production of a system of polymers between which, theoretically, no covalent bonds exist, the respective chains remaining held in place by means of permanent physical entanglements produced by the interweaving of the component polymer networks[1].

The methods of IPN preparation include sequential[2–4] and simultaneous polymerizations[4–6]. In sequential synthesis, the polymer I network is formed before monomer II is introduced, so polymer I restricts the extent to which the mixing of monomer II within polymer I can occur. The maximum incorporation of monomer II depends on the equilibrium swelling of polymer I. This imposes a limit on the range of compositions and hence properties that may be engineered by the sequential synthesis route. When the networks are synthesized simultaneously, however, the intermixing of the respective chemicals prior to polymerization ensures that the best random distribution of monomers is achieved, this distribution becoming fixed upon the polymerization and crosslinking of each component. Furthermore, the simultaneous route enables a wider range of compositions to be produced. The observed morphology of the IPN is dependent upon the compatibility of the materials combined, the relative rates of reaction and the respective quantities of each constituent present[7–9].

Two types of IPN may be formed depending on whether the polymer components are crosslinked or not; a full-IPN is said to be formed when both the components are crosslinked and a semi- or pseudo-IPN when only one of the components is crosslinked. A further subdivision is possible. When the host polymer (polymer I) is crosslinked and polymer II remains linear then a semi-I IPN is said to be formed. Conversely, a semi-II IPN results if polymer I is linear and polymer II is crosslinked.

Literature[6,10,11] shows that the combination of a glassy polymer with another which is rubbery at room temperature can produce IPNs possessing a range of properties depending upon which component forms the continuous matrix. IPNs therefore may be produced which exhibit a range of properties from reinforced elastomers to rubber reinforced high-impact plastics[9].

The present work examines the dynamic and the static mechanical properties of a range of sequential and simultaneous IPNs based on compatible polymers of polyurethane (PU) and poly(methyl methacrylate) (PMMA). The aim is to elucidate the factors which influence the IPN properties and to examine the presence of synergism in these properties.

* To whom correspondence should be addressed

0032-3861/93/091865-09

EXPERIMENTAL

Raw materials

The raw materials used are described in *Table 1*. The PU sheets were donated by B & T Polymers, Donald Macpherson's and Co. Ltd, and the remaining reactants were supplied by BDH Chemicals Ltd. Prior to IPN preparations the methyl methacrylate (MMA) monomer was freed from inhibitor by washing first with aqueous sodium hydroxide, then with distilled water, followed by drying over anhydrous calcium chloride. The PU sheets were dried prior to use by placing in a vacuum oven at 40°C for 24 h. All other chemicals were used as supplied.

Preparation of material systems

Sequential full-IPNs. The dried PU sheets (113 × 51 × 3 mm) were weighed and then immersed in inhibitor-free MMA containing 0.5% w/w 2,2'-azobisisobutyronitrile (AIBN) and 0.3 mol% crosslinking agent (ethylene glycol dimethacrylate, EGDMA) for varying periods of time (15 min–3 h). After the sheets had achieved the required percentage increase in weight, they were removed, blot dried and clamped between glass plates which were sprayed with silicon mould release agent. The assemblage was then wrapped in polythene and left for 20 h at room temperature in order to facilitate uniform monomer diffusion. Subsequently the sheets were heated at 60°C for 23 h, followed by 2.5 h at 80°C and 1 h at 100°C for MMA polymerization. The polymerized sheets were allowed to cool down to room temperature prior to demoulding, wiped clean of release agent, and left for 2 weeks at room temperature to drive off any unreacted MMA.

PMMA preparation. A linear MMA prepolymer was formed by heating inhibitor-free monomer with 0.5% w/w initiator AIBN in a water bath at 60°C until it had become noticeably viscous. Following the removal of the reaction exotherm by immersion in an ice bath for 30 min, the prepolymer was cast in a glass cell consisting of two clean dry glass plates separated by a rubber gasket (cellulose dialysis tubing pulled over rubber tubing) and held together by means of spring clips. The PMMA polymerization was completed by heating at 80°C for 2.5 h and at 100°C for 1 h.

The reaction mixture for crosslinked PMMA included 0.3 mol% crosslinking agent (EGDMA) which had to be first freed from its inhibitor by reduced pressure distillation (60°C, ~1 mm Hg). The distillate was stored in a refrigerator until required.

Table 1 Raw materials

Designation	Description
PU sheets	Base elastomer consisting of 400 and 2000 molecular weight polyoxypropylene glycol mixture reacted with a semi-pure MDI with a functionality of 2.3
Urethane polyols	A mixture of 400 and 2000 molecular weight polyoxypropylene glycol with OH values of 275 and 55, respectively
Urethane crosslinking agent	Trimethylol propane
MDI	A semi-pure diphenylmethane diisocyanate with a functionality of 2.3 and NCO content of 27.6%
Organomercury catalyst	Phenylmercuric ethanoate
MMA	Methyl methacrylate
EGDMA	Ethylene glycol dimethacrylate
AIBN	2,2'-Azobisisobutyronitrile

Simultaneous IPNs were synthesized by mixing together appropriate amounts of the urethane polyols with 0.7 wt% organo-mercury catalyst and the PMMA reagents (these were monomer MMA and 0.5% w/w AIBN for semi-IPN, and also 0.3 mol% EGDMA for full-IPN preparation). The mixture of urethane polyols was at a ratio of 5 × (high molecular weight polyol) to 1 × (low molecular weight polyol). The reagents were well mixed and MDI was added at a molar ratio of NCO/OH = 1.07/1. The final mixture was degassed and cast into moulds. The filled moulds were left at room temperature for 30 min, then heated to 60°C and held for 23 h, followed by 2.5 h at 80°C and 1 h at 100°C for MMA polymerization. The polymerized IPN sheets were allowed to cool down to room temperature prior to demoulding. Additional information on the preparation and reaction progress of PU and simultaneous IPNs is presented elsewhere[12].

The simultaneous IPN formation involved the synthesis of both polymers from their chemical constituents. However, the method is more accurately *in situ* sequential synthesis, since the networks do not gel simultaneously. There is effectively a two-step process, such that PU gelation and formation occurs first followed by PMMA formation. Nevertheless, the IPNs produced in this way are still thought to possess a higher degree of interpenetration than the ones obtained by a strictly sequential method.

Test methods

Dynamic mechanical data were obtained using a Du Pont 983 dynamic mechanical analyser in resonant frequency mode over a temperature range from −80 to 160°C at a heating rate of 4°C min^{-1}. Test pieces were ~10 mm wide and the clamp separations were adjusted according to the stiffness of the specimens. Wider clamp settings are required for the stiffer and/or thicker specimens. The amplitude (peak-to-peak) of sinusoidal oscillations, mostly 0.3–0.6 mm, were also chosen according to the stiffness and thickness of the specimens.

Tensile testing was performed at room temperature using an Instron tensometer (model no. 1026) in accordance with ASTM D 638M at a cross-head speed of 50 mm min^{-1}.

Hardness testing was performed according to ASTM D 2240-85 using a type D Shore durometer.

Notched specimens were impact tested in a three-point bending mode, 40 mm span, using an instrumented falling weight machine, fitted with a chisel-shaped striker of angle 30° and tip radius 1.5 mm, at 1 m s^{-1} impact speed. The test pieces (3.5 × 10 × 60 mm) were notched to ~1 mm depth by milling with a cutter of angle 45° and tip radius 0.25 mm. They were then frozen by immersion in liquid nitrogen and were allowed to reach either −50 or −10°C immediately prior to impact. Impact tests were conducted at −50°C, i.e. below the glass transition temperature (T_g) of the materials, where it was expected that any vulnerability would be indicated and hence the evaluation be more appropriate.

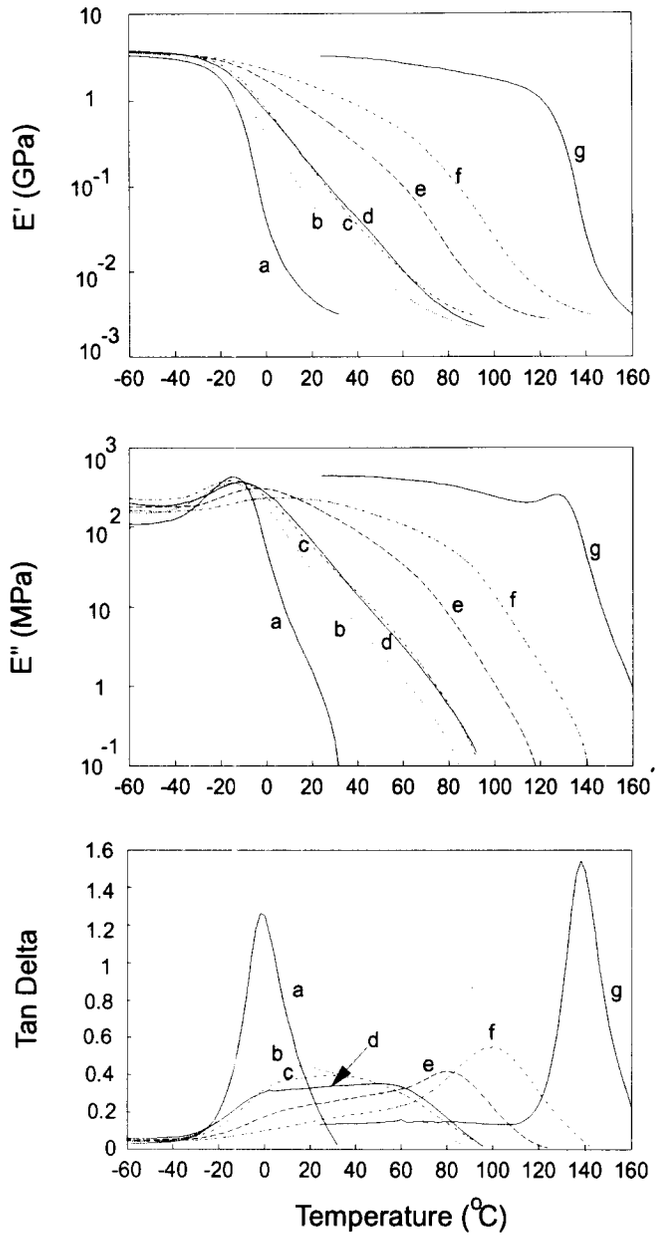

Figure 1 Dynamic mechanical properties for sequential full-IPNs with PU/PMMA compositions: (a) 100/0; (b) 82/18; (c) 71/29; (d) 66/34; (e) 60/40; (f) 40/60; (g) 0/100

The fractured surfaces of the impact test pieces were platinum sputter-coated and examined by scanning electron microscopy (SEM).

The abrasion resistance was determined using a Taber Dyne Table (model 505) with CS-10 abrasion wheels. The samples were cut into segments of a disc of radius 50 mm, weighed accurately, placed adjacently on the abrasion table and were abraded under 1 kg load for 3000 cycles at 70 rev min^{-1}. The abraded samples were re-weighed and the material loss recorded.

RESULTS AND DISCUSSION

Dynamic mechanical properties

Figures 1–3 show the dynamic mechanical behaviour of sequential and simultaneous IPNs and those of the component polymers. The IPNs produced broad transitions of various types depending on the composition. The analysis of transition broadening and the patterns of behaviour of the dynamic mechanical properties, storage modulus (E'), loss modulus (E'') and damping term ($\tan\delta$), during transition are fully covered elsewhere[13,14]. The plots clearly show that at the extreme IPN compositions, i.e. PU/PMMA ratios of 80/20 and 20/80, single relatively sharp $\tan\delta$ curves were obtained and at the intermediate IPN compositions broad $\tan\delta$ curves were obtained. This makes the determination of the T_g based on $\tan\delta$ less definitive for the mid-range IPNs. The T_g values presented in *Figure 4* are mostly the temperatures of $\tan\delta$ maxima. In the case of the IPNs with almost rectangular $\tan\delta$ peaks, the temperature coinciding with the centre of the $\tan\delta$ peak span was considered as the T_g. *Figure 4* shows a rapid increase in T_g above 30% PMMA, where, perhaps, the PMMA phase becomes continuous or reaches a sufficient level to influence the T_g. This is corroborated by the results of the various mechanical properties discussed below.

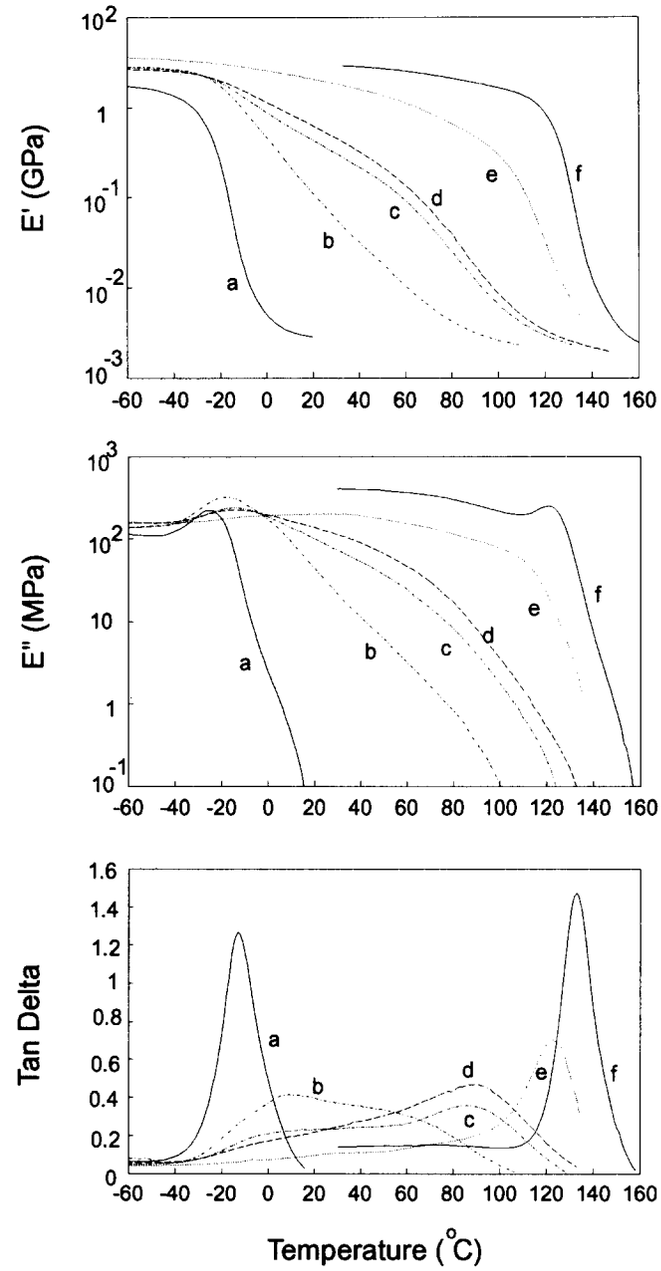

Figure 2 Dynamic mechanical properties for simultaneous semi-I IPNs with PU/PMMA compositions: (a) 100/0; (b) 70/30; (c) 55/45; (d) 50/50; (e) 20/80; (f) 0/100

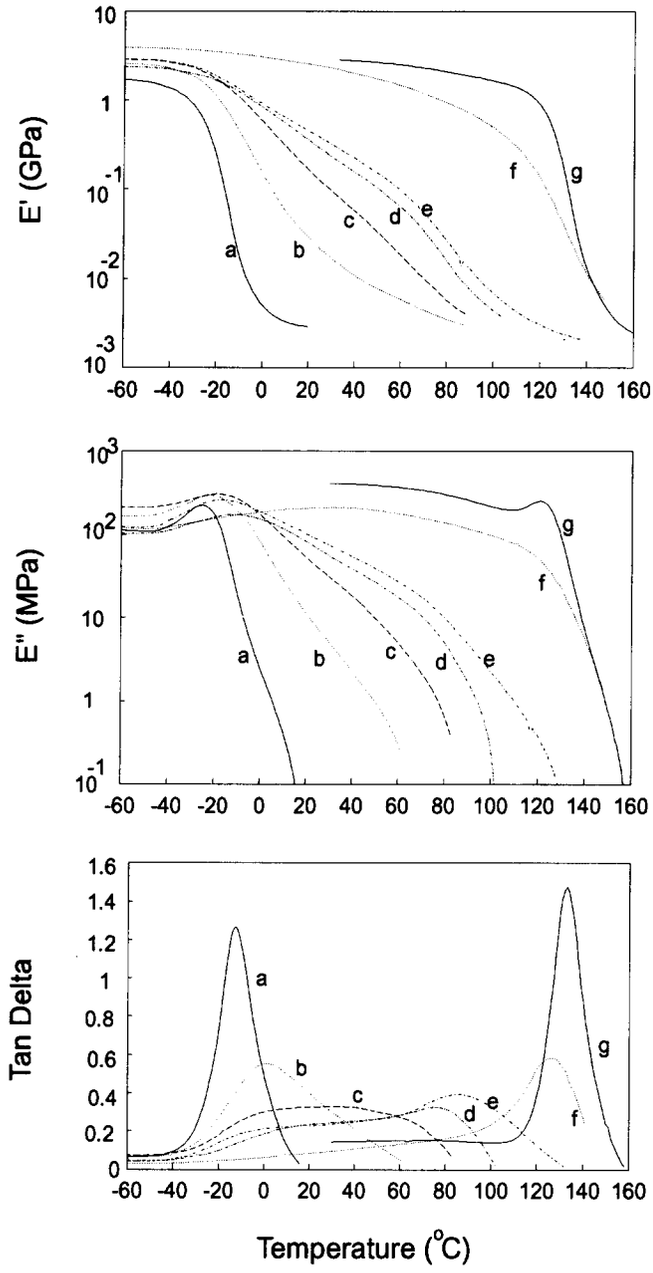

Figure 3 Dynamic mechanical properties for simultaneous full-IPNs with PU/PMMA compositions: (a) 100/0; (b) 80/20; (c) 70/30; (d) 60/40; (e) 50/50; (f) 20/80; (g) 0/100

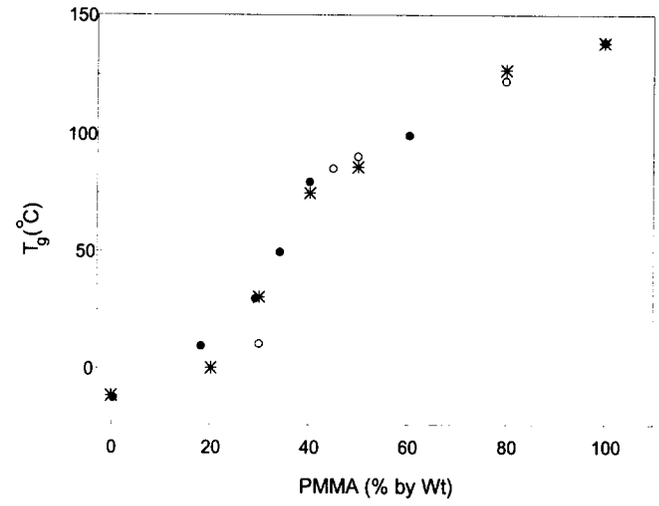

Figure 4 Glass transition temperature (based on tan δ peak temperatures) *versus* composition for: (*) simultaneous full-IPNs; (○) simultaneous semi-I IPNs; (●) sequential full-IPNs

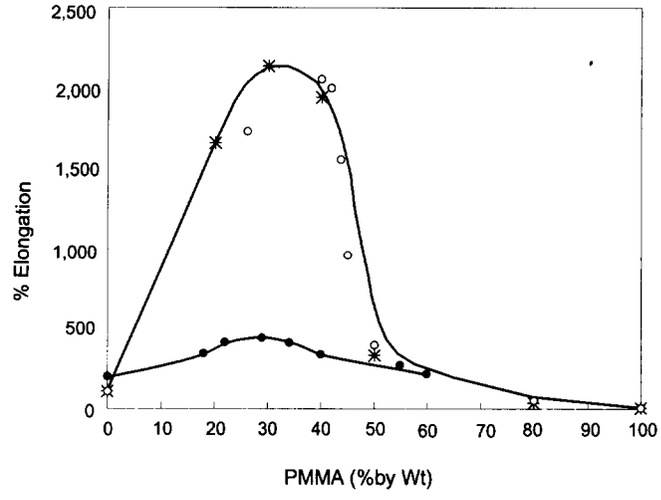

Figure 5 Elongation to failure *versus* composition for: (*) simultaneous full-IPNs; (○) simultaneous semi-I IPNs; (●) sequential full-IPNs

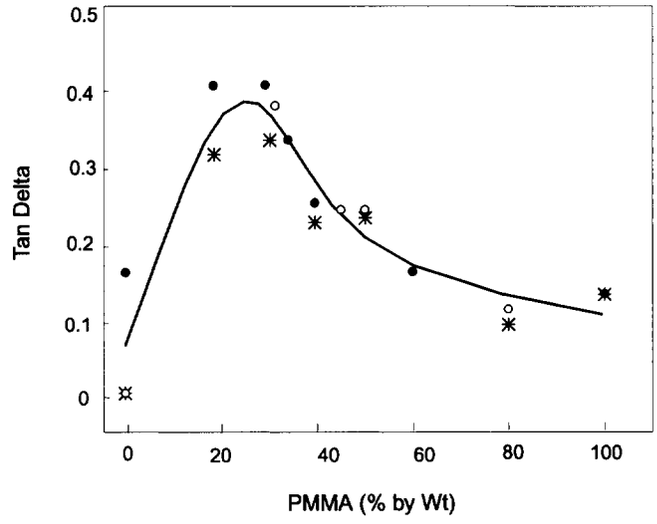

Figure 6 Tan δ (values taken at 25°C) *versus* composition for: (*) simultaneous full-IPNs; (○) simultaneous semi-I IPNs; (●) sequential full-IPNs

Mechanical properties

Tensile elongation and impact. Mechanical properties which rely on the capacity of the material to undergo molecular relaxation and thus dissipate energy will be influenced by tan δ values at test temperatures. There was, therefore, a close correlation between the percentage elongation to failure and the damping (tan δ) values at room temperature (cf. *Figures 5* and *6*). Tan δ values corresponding to 25°C were extracted from *Figures 1* to *3*. Both the properties went through a maximum at an IPN composition of ~70/30 (PU/PMMA). However, there was considerable variation in the maximum elongation values exhibited by the simultaneous and the sequential systems. Unusually high percentage elongation values (~2000%) were obtained with the simultaneous IPNs. This can only be attributed to the possibility that much more effective levels of intermolecular mixing were achieved by simultaneous synthesis and the resultant

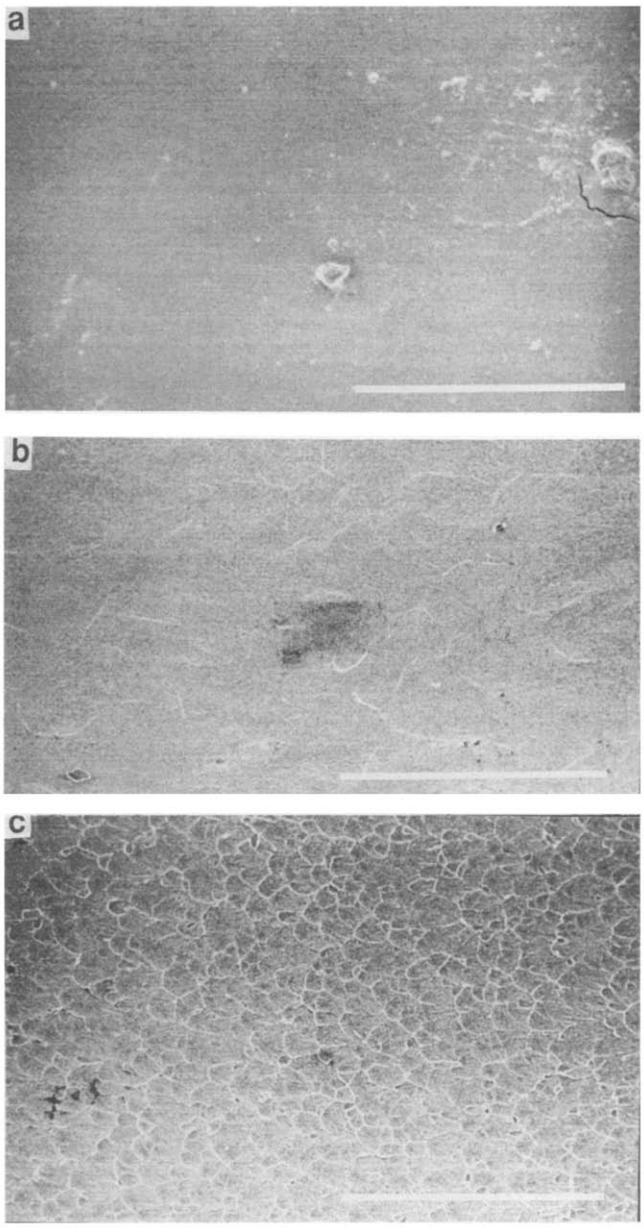

Figure 7 SEM micrographs of the fracture surfaces of the simultaneous full-IPN specimens impact tested at −50°C: (a) 70/30; (b) 50/50; (c) 20/80 PU/PMMA. Scale bar = 100 μm

IPNs, hence, experienced a uniform distribution of stress when loaded. Further information to elucidate the extent of homogeneity in IPNs may be obtained from an examination of the impact fracture surface micrographs. The impact tests were conducted at −50°C, below the T_g of PU, to ensure brittle failure for the elastomeric compositions. Under such cryogenic conditions smooth fracture surfaces will be expected from IPNs with uniform and intimate mixing between the component polymers. Conversely, an appearance of separate phases or material agglomerates can be expected on the fracture surfaces of less thorough and non-uniform IPN mixes. In simultaneous IPNs up to a composition ratio of 50/50, smooth fracture surfaces were experienced as in *Figures 7* and *8*. These are similar to the PU fracture surface (see *Figure 9a*) with no evidence of PMMA-rich regions and with all the appearance of a single-phase material. At simultaneous IPN compositions of 50/50 and above, the fracture surfaces (*Figures 7* and *8*) gradually assumed the appearance of the PMMA fracture surface seen in *Figure 9b*, where surface markings were scale-like. These IPN surfaces were also of uniform appearance, implying the intimacy of the mixing between the component polymers. However, in sequential IPNs the non-uniformity of interpenetration can be seen from the respective fracture micrographs (*Figure 10*), where PMMA aggregates are clearly visible in all the IPN formulations. Uneven distribution of PMMA can give rise to stress concentration, particularly in the regions where large amounts of PMMA are segregated out, and cause premature failure of the material under load. Thus, in sequential IPNs, the lack of sufficiently uniform mixing of the polymers can result in premature failures after moderate elongations compared to simultaneous IPNs.

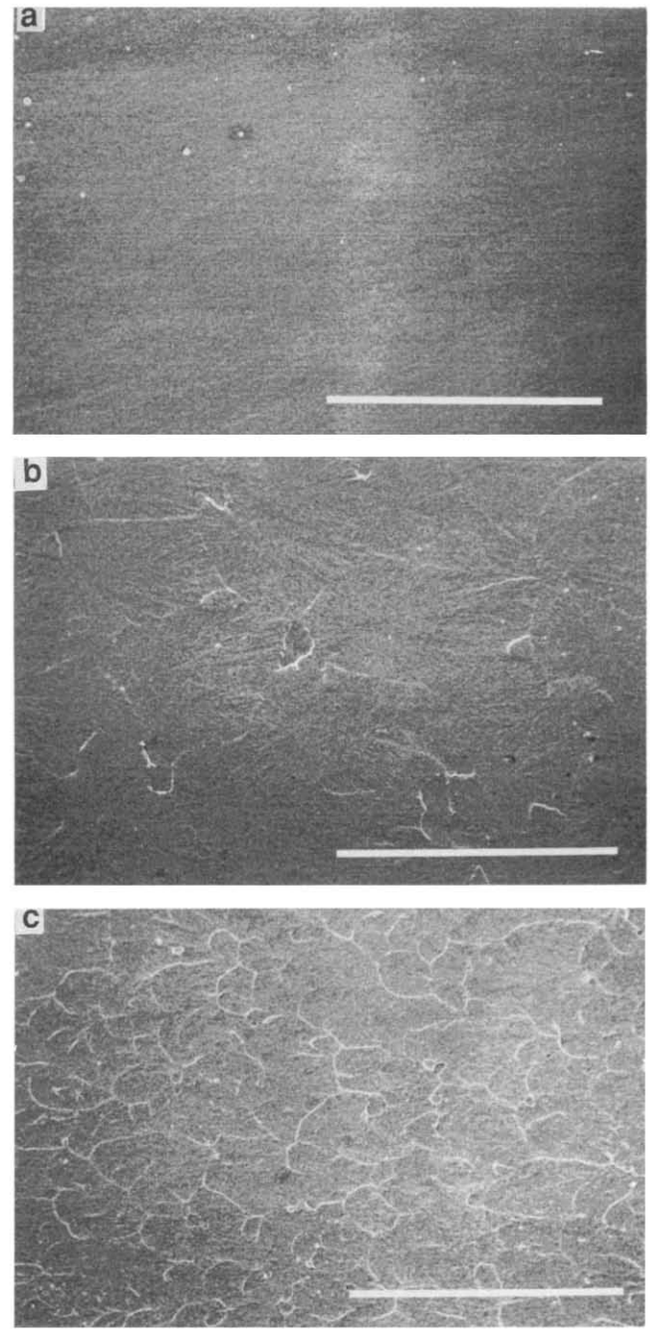

Figure 8 SEM micrographs of the fracture surfaces of the simultaneous semi-I IPN specimens impact tested at −50°C: (a) 70/30; (b) 50/50; (c) 20/80 PU/PMMA. Scale bar = 100 μm

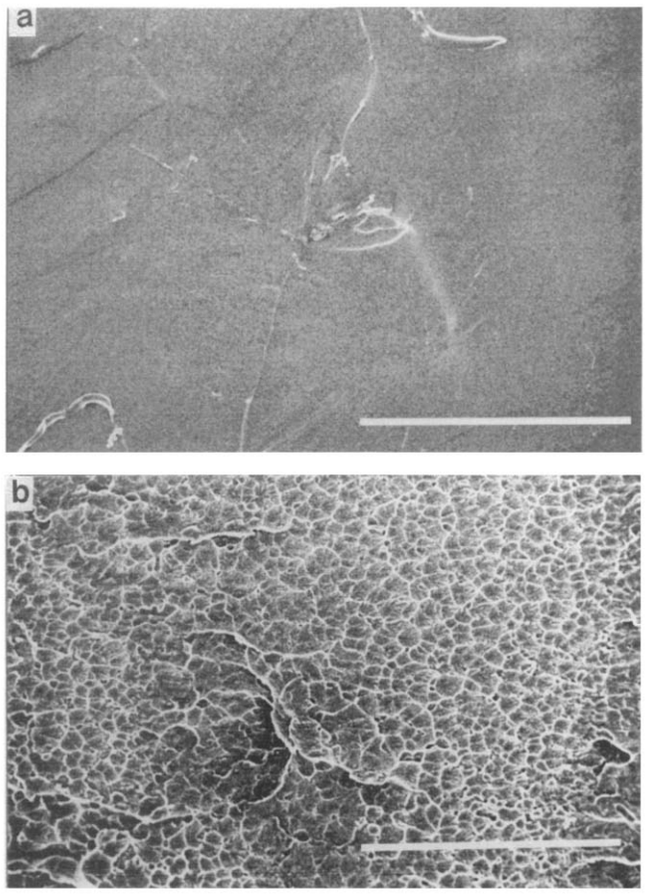

Figure 9 SEM micrographs of the fracture surfaces of (a) PU and (b) crosslinked PMMA specimens impact tested at −50°C. Scale bar = 100 μm

The impact strength of the simultaneous IPNs at −50°C showed no significant reductions from the PU value up to ~50% PMMA but deteriorated with further increases in PMMA content as in *Figure 11*. An associated transition in the fracture surface morphology was also observed. The fracture surfaces of the IPNs up to 50% PMMA content remained plain as influenced by PU, but thereafter exhibited special markings associated with PMMA (see *Figures 7* and *8*).

Comparison of *Figures 7c* and *8c* shows that simultaneous full-IPNs, where PMMA is crosslinked, exhibit a greater intensity of the surface markings than the semi-I IPNs, composed of linear PMMA. The impact strength of the sequential IPNs, at −50°C, indicated an almost linear drop with increasing PMMA.

Some of the impact tests were conducted at −10°C, around the T_g of the PU component, and thus significant improvements were observed with increasing PU content. The associated fracture micrographs showed rough fracture surfaces, as in *Figure 12*, consistent with more ductile failures.

Elastic modulus and hardness. The static elastic moduli values for the simultaneous IPNs showed a sigmoidal variation with composition when plotted on a logarithmic scale (*Figure 13*). A rapid increase in the elastic modulus was observed between the PU/PMMA ratios of ~70/30 to 30/70. This pattern of behaviour has been attributed to the occurrence of phase inversion in polymer blends[15,16]. Thus, on such a premise, the PMMA phase becomes continuous when it is 30% w/w and co-continuity is maintained to ~30/70 (PU/PMMA) composition followed by a dispersion of PU in PMMA.

A model[17] based on equation (1), which predicts phase inversion in two-component polymer systems, is consistent with simultaneous IPN data (as in *Figure 13*):

$$w_1/\{1+\varepsilon[(E_1/E)-1]\}+w_2/\{1+\varepsilon[(E_2/E)-1]\}=1 \quad (1)$$

where $\varepsilon=2(4-5\nu)/15(1-\nu)$, ν is Poisson's ratio, w is the weight fraction, E is the elastic modulus and subscripts 1 and 2 represent the component polymers. Here, ν is assumed to be 0.4.

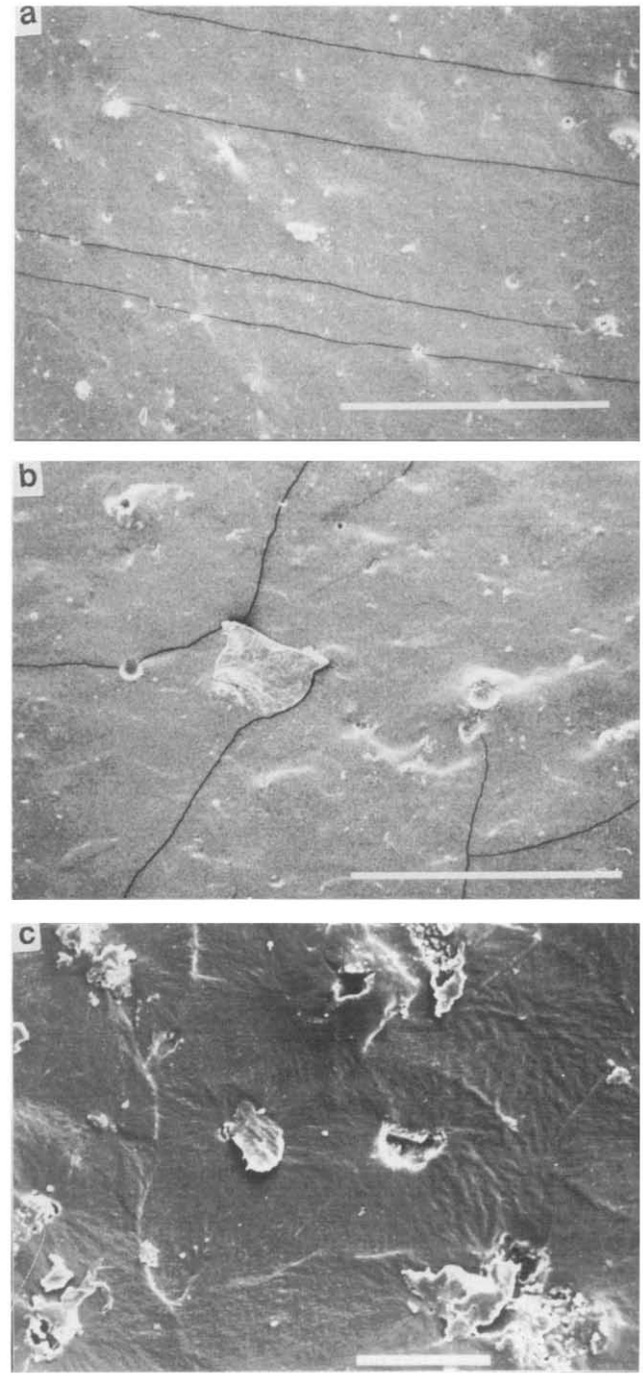

Figure 10 SEM micrographs of the fracture surfaces of the sequential full-IPN specimens impact tested at −50°C: (a) 70/30; (b) 60/40; (c) 45/55 PU/PMMA. Scale bar = 100 μm for (a) and (b) and 10 μm for (c)

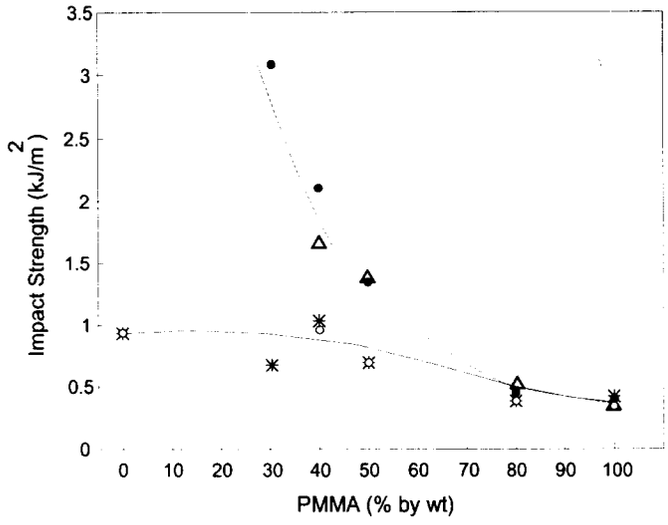

Figure 11 Impact energy at failure per cross-sectional area *versus* PMMA content for simultaneous (*, ●) full-IPNs and (○, △) semi-I IPNs. Impact tested at (——) −50°C and (----) −10°C

Figure 12 SEM micrograph of the fracture surface of the 70/30 simultaneous full-IPN specimen impact tested at −10°C. Scale bar = 100 μm

This model has been previously applied to simultaneous PU/PMMA IPNs with varying degrees of success. It has been shown to describe accurately the work by Kim *et al.*[18], where the occurrence of phase inversion was established by electron microscopy.

Allen *et al.*[19] have found that a dual-phase continuity model, related to the equation of Davies[20] [equation (2)], corresponded to the dynamic shear moduli data of their simultaneous PU/PMMA IPNs much better than that related to equation (1). This led to the conclusion that these materials had dual-phase continuity:

$$E^{0.2} = w_1 E_1^{0.2} + w_2 E_2^{0.2} \quad (2)$$

It is shown in *Figure 14* that the curve due to equation (2) fits the elastic moduli data of the sequential full-IPNs, suggesting the existence of a dual-phase continuity. In another study[21] on sequential full-styrene-butadiene rubber/polystyrene, equation (2) has been found to predict best the elastic modulus values over the range of compositions. Appropriately, dual-phase continuity was observed in these IPNs under transmission electron microscopy.

The room temperature dynamic real moduli values were, as expected, greater than the static elastic moduli values (cf. *Figures 13* and *14* with *Figure 15*). The IPNs, particularly those with higher PU content, appear to show increased stiffening under dynamic conditions, and the resultant E' values for both sequential and simultaneous systems follow a curve similar to the one predicted by equation (2). However, because of the frequency effect on elastic modulus, it will be inappropriate to draw any conclusions as regards the continuity of the phases by the pattern of behaviour of the dynamic modulus. Hardness values also vary in a sigmoidal fashion as seen in *Figure 16*, the highest rate of change occurring between 30% and 70% PMMA contents where the phases are assumed to display co-continuity. However, the hardness data presented here must be qualified by explaining that the measurements become less reliable at the outer ranges of the Shore-meter scale.

Ultimate tensile strength and abrasion resistance. The ultimate tensile strength (*Figure 17*) was found to increase,

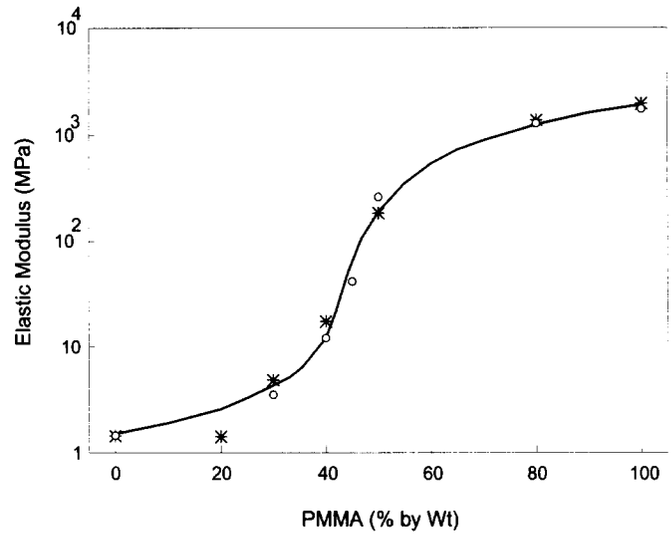

Figure 13 Elastic modulus (log scale) *versus* composition for simultaneous (*) full-IPNs and (○) semi-I IPNs. The solid line is based on equation (1)

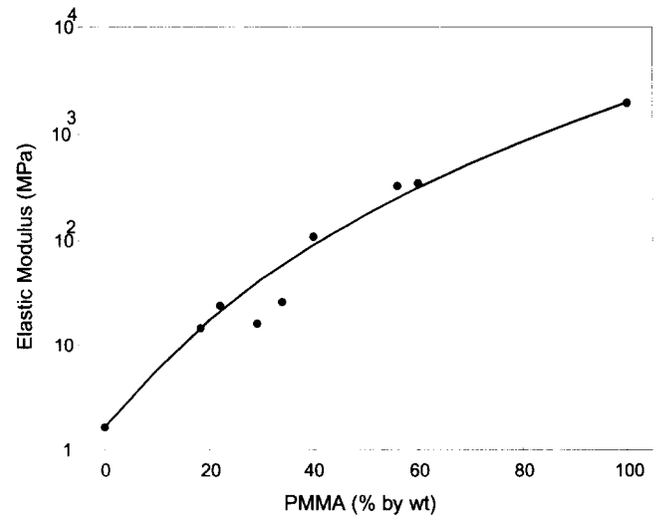

Figure 14 Elastic modulus (log scale) *versus* composition for sequential full-IPNs. The solid line is based on equation (2)

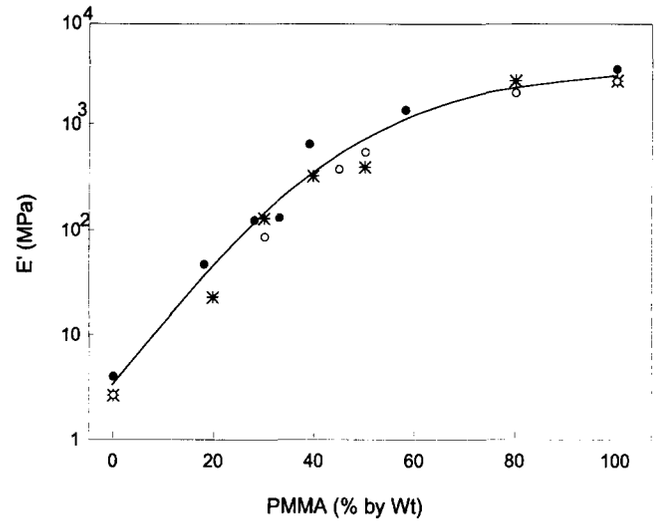

Figure 15 Dynamic real modulus (log scale) (values taken at 25°C) *versus* composition for: (*) simultaneous full-IPNs; (○) simultaneous semi-I IPNs; (●) sequential full-IPNs

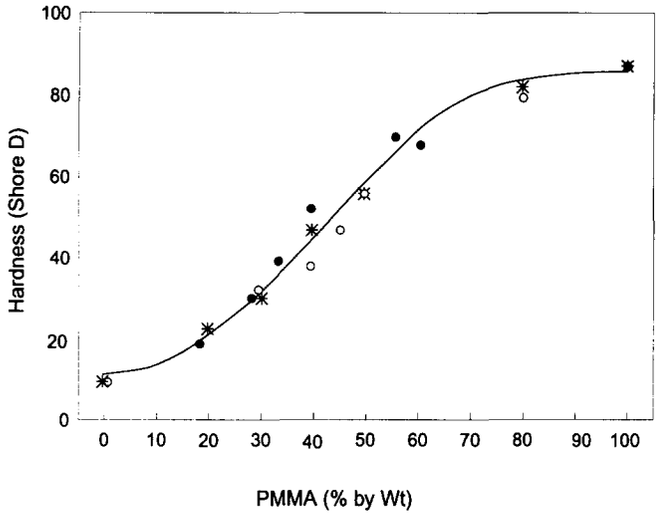

Figure 16 Hardness *versus* composition for: (*) simultaneous full-IPNs; (○) simultaneous semi-I IPNs; (●) sequential full-IPNs

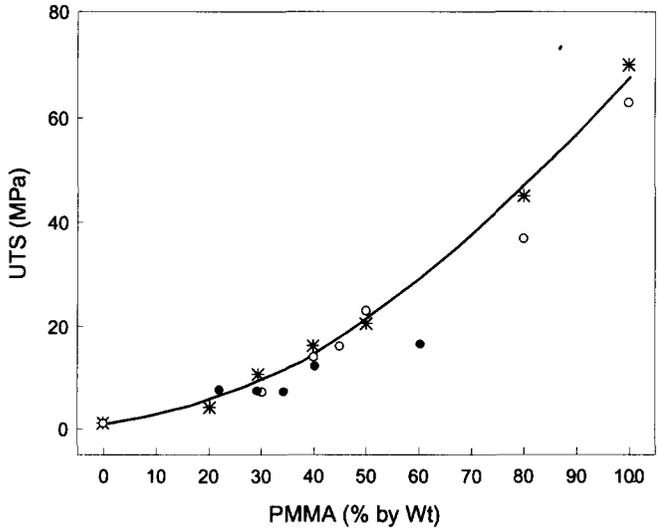

Figure 17 Ultimate tensile strength (UTS) *versus* composition for: (*) simultaneous full-IPNs; (○) simultaneous semi-I IPNs; (●) sequential full-IPNs. The solid line is the best fit to the simultaneous data

Table 2 PMMA contents (%) for maximum property improvement in IPNs

	% PMMA required for synergy in:				
IPN type	Hardness	Impact	Elongation	T_g	Tan δ
Simultaneous	60–70	40	30–40	40	30
Sequential	60–70	No synergism	30–40	40	30

as expected, with increasing PMMA content, although not at a uniform rate. The rise in ultimate tensile strength appears to occur in two stages: a limited climb up to 30% PMMA, followed by a more rapid increase with additional PMMA.

It can also be seen from *Figure 17* that the simultaneous formulations on the whole are stronger than the sequential ones. This is contributed to by unusually large percentage elongations to failure exhibited by the simultaneous IPNs.

Abrasion resistance of PU and sequential IPNs was measured and the IPNs across the composition range were found to withstand increased abrasion compared to PU. Material losses of ~14 and 7 mg were recorded for PU and IPNs (within the PU/PMMA range 70/30 to 40/60), respectively. This improvement is effected by the increased hardness and tensile strength in the IPN systems.

Finally, it can be demonstrated that the interpenetration of PU and PMMA polymers produces synergism in most of the properties considered here. The room temperature values of the IPN properties were found to increase at certain compositions beyond the weighted average value of the properties of the component polymers. The compositions at which maximum synergism was observed in various properties are presented in *Table 2*. Maximum synergism appears to occur mainly in the PU/PMMA composition range of 30/70 to 40/60. In the case of hardness, the maximum deviation from the computed average occurs at ~65% PMMA content.

CONCLUSIONS

1. Broad tan δ peaks with almost constant amplitudes over wide temperature ranges are exhibited by the intermediate range compositions of PU and PMMA IPNs.
2. A correlation exists between the elongation to failure and the magnitude of damping (measured by tan δ): maxima are observed in the room temperature values of these properties at identical IPN compositions.
3. The impact strengths of the simultaneous IPNs at −50°C remain the same as the PU value up to 50% PMMA content but suffer reductions with further increases in PMMA. The fracture surface morphology also shows a transition at 50/50 PU/PMMA composition from a PU- to a PMMA-dominant appearance. The impact strength of the sequential IPNs at −50°C decreases almost linearly with increasing PMMA content. At −10°C, as expected, the fracture is more ductile and the impact strength improves considerably with increasing PU content.
4. The elastic modulus, hardness and the tensile strength of IPNs increase with increasing PMMA content. The patterns of variation and the extent of improvements differ between the simultaneous and the sequential

systems. The plots of elastic modulus *versus* IPN composition comply with a phase inversion model for the simultaneous IPNs and with a dual-phase continuity model for the sequential IPNs.

5. The distribution of the component polymers in the simultaneous IPNs appears to be more homogeneous than in the sequential IPNs. Much higher elongations to failure and greater tensile strengths are indicated by the simultaneous systems.
6. The abrasion resistance of PUs may be significantly improved by interpenetration with PMMA.
7. IPN formulations can produce synergism in properties such as hardness, impact strength, elongation to failure, T_g and mechanical damping. Maximum property improvements are experienced mostly in the PU/PMMA composition range of ~30/70 to 40/60.

ACKNOWLEDGEMENTS

The authors wish to thank B & T Polymers, Donald Macpherson's and Co. Ltd, and, in particular, Mr D. Drury, for support. We are also grateful to Mrs M. Young for her help in preparing the manuscript.

REFERENCES

1 Klempner, D., Frisch, K. and Frisch, H. *J. Elastoplast.* 1973, **5**, 196
2 Sperling, L., Taylor, D., Kirkpatrick, M. and George, H. *J. Appl. Polym. Sci.* 1970, **14**, 73
3 Gesner, B. in 'Encyclopedia of Polymer Science and Technology', (Eds H. F. Mark, N. G. Gaylord and N. M. Bikales), Interscience Publishers, New York, Vol. 10, 1968, p. 694
4 Brandrup, J. and Immergut, E. 'Polymer Handbook', Wiley-Interscience, New York, 1975
5 Olabisi, O., Robeson, L. and Shaw, M. 'Polymer–Polymer Miscibility', Academic Press, New York, 1977
6 Frisch, K., Klempner, D. and Migdal, S. *J. Polym. Sci., Polym. Chem. Edn* 1974, **12**, 885
7 Touhsaent, R. E., Thomas, D. A. and Sperling, L. H. *J. Polym. Sci. C* 1974, **46**, 175
8 Klempner, D., Berkowski, L., Frisch, K., Hsieh, K. and Ting, R. *Polym. Mater. Sci. Eng.* 1985, **52**, 57
9 Kim, S., Klempner, D., Frisch, K., Frisch, H. and Radigan, W. *Macromolecules* 1976, **9**, 258
10 Sperling, L. *Polym. Eng. Sci.* 1985, **25**, 517
11 Frisch, H. and Klempner, D. *Polym. Sci. Technol.* 1980, **11**, 203
12 Rollins, S. N. *PhD Thesis* University of Ulster at Jordanstown, 1990
13 Akay, M., Rollins, S. N. and Riordan, E. *Polymer* 1988, **29**, 37
14 Akay, M. and Rollins, S. N. *Polymer* 1993, **34**, 967
15 Nielsen, L. E. 'Mechanical Properties of Polymers and Composites', Marcel Dekker, New York, 1974, Ch. 7
16 Sperling, L. H. 'Interpenetrating Polymer Networks and Related Materials', Plenum Press, New York, 1981
17 Budiansky, B. *J. Mech. Phys. Solids* 1965, **13**, 223
18 Kim, S., Klempner, D., Frisch, K. and Frisch, H. *Macromolecules* 1977, **10**, 1187
19 Allen, G., Bowden, M. J., Todd, S. M., Blundell, D. J., Jeffs, G. M. and Davies, W. E. A. *Polymer* 1974, **15**, 28
20 Davies, W. E. A. *J. Phys. D* 1971, **4**, 318
21 Donatelli, A. A., Sperling, L. H. and Thomas, D. A. *Macromolecules* 1976, **9**, 671